Volume 7, Issue 11, November – 2022 International Journal of Innovative Science and Research Technology
ISSN No:-2456-2165

A Review of GHG Emission Reduction Techniques that Incorporate Post-Combustion CO2 Capture using Carbon Fiber Monolithic Adsorbents from Flue Gas

Cherrie Lyn Villanueva
Feati University: Civil Engineering Department
Philippine Institute of Civil Engineers
Sta. Cruz Manila, Philippines

Cherrie Lyn Villanueva
Research Development Group
Innostrukt Company
Pasay City, Philippines

Abstract:- Technology for capturing carbon dioxide (CO2) has been applied in industry for more than 80 years

[7.]. In this study the usage of CO2 separation units will be facilitated by extensive knowledge in the carbon capture procedures and different applications of CO2 [7.].

As the production of carbon dioxide (CO2) is a byproduct of burning fossil fuels, effective CO2 capture from industrial and commercial operations is seen as a key method with the potential to significantly lower atmospheric CO2 levels [2.].

[66.] The three primary types of capture now in use are oxy-fuel combustion, pre-combustion capture, and post-combustion capture. The fossil fuel is pre-combusted with air or oxygen and partially oxidized to produce CO and H2 [2.]. The result of this reaction with steam is a mixture of CO2 and additional H2. Before combustion occurs, the carbon dioxide is eliminated and the H2 can be used as fuel. Oxy-combustion is the process of burning oxygen rather than air, which produces [2.] a flue gas that is primarily pure CO2 and may be appropriate for storage. In post combustion capture, CO2 is extracted from the flue gas produced when fossil fuels are burned. The post combustion capture (PCC) technology offers a way for [12.] stationary fossil fuel-fired power plants, both new and old, to absorb CO2 in the near future without having to make significant changes to their current combustion processes and infrastructure.

This study categorizes current and emerging [71.] post-combustion CO2 capture systems, evaluates CO2 capture techniques, and contrasts their properties. The report then investigates pertinent [12.] studies on carbon fiber composite adsorbents from flue gas for CO2 capture and goes into detail about the adsorbents' production characteristics and CO2 adsorption performance. Next, the paper discusses potential system configurations for this procedure in the future for commercial purposes.

Experiments were performed utilizing simulated flue gas in a [3.] 2.0 m long, big sized adsorption column to assess the use of [33.] large honeycomb structured monolithic carbon fiber composites (HMCFC) to CO2 capture. At room temperature and pressure, the HMCFC's mass absorption capability for pure CO2 was 11.9 wt% on average. [29.] The CO2 capture efficiency during the adsorption breakthrough research was determined to be over 98% with a simulated flue gas made up of [3.] 13 vol% CO2 (partial pressure 13 kPa), 5.5% O2, and the remaining N2 at 298K.

Thermal regeneration after adsorption at [3.] 398 K without an inert gas purge to recover the adsorbed gas produced a desorbed CO2 gas concentration of up to 100% [3.] but with a CO2 recovery whereas vacuum regeneration (up to 30 kPa) produced less than 5% CO2 and less than 20% CO2. To obtain extremely high CO2 recovery and purity, coupled heat and [3.] vacuum regeneration was discovered to be a successful CO2 desorption approach. Additionally, more concentrated CO2 was obtained in the desorbed gas [3.] when the adsorbents were flushed with a certain amount of CO2 following the flue gas adsorption process. The desorbed gas showed a 100% CO2 content under ideal working conditions, with a recovery rate of over 97% from the input flue gas. During regeneration trials with repeated heating and cooling, [3.] the carbon fiber composite adsorbents shown very good mechanical stability and were unaffected by water from moisture condensation.

I. INTRODUCTION

[26.] Emissions of greenhouse gases (GHGs) are currently [5.] one of the biggest problems facing societies all over the world. Carbon Dioxide, Methane, Nitrous Oxide, Chlorofluorocarbon-12 (CFC-12), and Ozone are the main GHGs. In 2018, there were 51.8 Gt CO2e of human emissions in the world (Aslani et al., 2014) .

Human activities like the use of fossil fuels for transportation, industrial processes, and the generation of heat and electricity are the main cause [5.]of GHG emissions (Sources of Greenhouse Gas). Some of the effects of these emissions and a lack of conservation include the [5.] melting of the polar ice caps and glaciers, rising ocean levels, floods, drier and warmer climates, the extinction of diverse plant and animal species, a negative impact on food production, and a lack of clean water supplies are some of the negative effects caused by these emissions and the fact that they are not within our control (Effects | Facts - Climate). Even by [58.] limiting global warming to 2 °C, the consequences of these emissions on the ecosystem and the world [7.]cannot be minimized (Carbon capture technology, 2017)

There are numerous ways to lower GHG emissions. Three crucial tactics include using [7.]renewable energy sources, optimizing energy systems, and putting carbon-capturing devices in place (Fawzy et al., 2020).

CO2 [7.] is the main greenhouse gas that contributes to global warming. It is released into the atmosphere from a number of sources, primarily from the burning of fossil fuels used in manufacturing, transportation, and power generation. (Thiruven , 2009). Natural sinks like the [31.] weathering of rocks and the photosynthesis of carbon compounds by plants and marine plankton closely balance out natural sources over timescales longer than a few years, [25.] despite the fact that natural sources of carbon dioxide are more than 20 times greater than sources resulting from human activity (Thiruven , 2009). [19.] In the 10,000 years between the end of the last glacial maximum and the beginning of the industrial period, the [27.] atmospheric concentration of carbon dioxide had remained between 260 and 280 parts per million [27.] as a result of this equilibrium. The [2.] long-term effectiveness of these natural sinks in absorbing atmospheric CO2 has been observed to be deteriorating, according to (Canadell et al.) with significant consequences for the rise of atmospheric CO2 in the present and the future.

Since 1751, the combustion of fossil fuels and the manufacture of cement have contributed around [2.] 321 billion tons of carbon to the atmosphere. Since the middle of the 1970s, half of these emissions have taken place. Between 1971 and 2002, the world's CO2 emissions climbed by more than 70%. The generation of electricity is expected to [2.] account for about half of the increase in global emissions between 2000 and 2030 [2.] as both developed and developing nations [63.] demand for electricity is expected to rise. In 2004, the total emissions from burning fossil fuels were made up of 1434 million tons of carbon from the [68.] combustion of gaseous fuels, such as natural gas, and 6130 million tons of carbon from the burning of liquid and solid fuels [8]. The worldwide fossil year 2002. Estimated CO2 emissions are [2.] 6975 Mt of carbon (about 25,000 Mt of CO2).

A coordinated effort is required to stabilize the atmospheric level of CO2 due to the rising global energy demand, which is predicted to rise by [2.] two-thirds over the next 30 years with fossil fuels serving as the main source of energy. In recent years, CO2 capture and storage (CCS) has drawn a lot of interest and is now acknowledged [45.] as one of the most promising methods for reducing CO2 emissions. [2.] In particular, post combustion capture reduces the need for significant changes to the [2.] combustion process and offers a way for stationary fossil fuel-fired power plants, both new and old, to capture CO2 in the near future. According to some estimates, the cost of CO2 capture accounts for the majority (two-thirds) of the costs associated with the carbon sequestration process. As a result, one of the top priorities in the realm of CCS is the development of an effective and affordable CO2 collecting mechanism.

A CSIRO created honeycomb structured [11.] carbon fiber composite was described in our prior study (Thiruvenkatachari et al., 2009a). Through a laboratory-scale study, we examined the effects of fabrication process conditions on CO2 adsorption performance at ambient pressure and temperature. We discussed the fabrication process using various types of carbon fiber raw materials and CO2 adsorption capacities, compared their performance with [70.] that of commercial activated carbon adsorbents, and discussed the performance of the materials with commercial activated carbon.

II. TECHNOLOGY FOR CAPTURING CO2

Because [10.] CO2 is produced during combustion, the kind of combustion directly influences the best method for removing CO2 from the atmosphere. Although there are CO2 capture technologies on the market, they are often expensive and account for between 70 and [8.] 80 percent of the entire cost of a complete CCS system, which includes capture, transport, and storage (Blomen et al., 2017).

Therefore, substantial R&D efforts are concentrated on lowering operational costs and energy penalty. In relation to various combustion processes, [28.] there are three basic CO2 capture systems: post-combustion, pre-combustion, and oxyfuel combustion. Figure 1 illustrates three technologies. 1 and the sections that follow are covered.

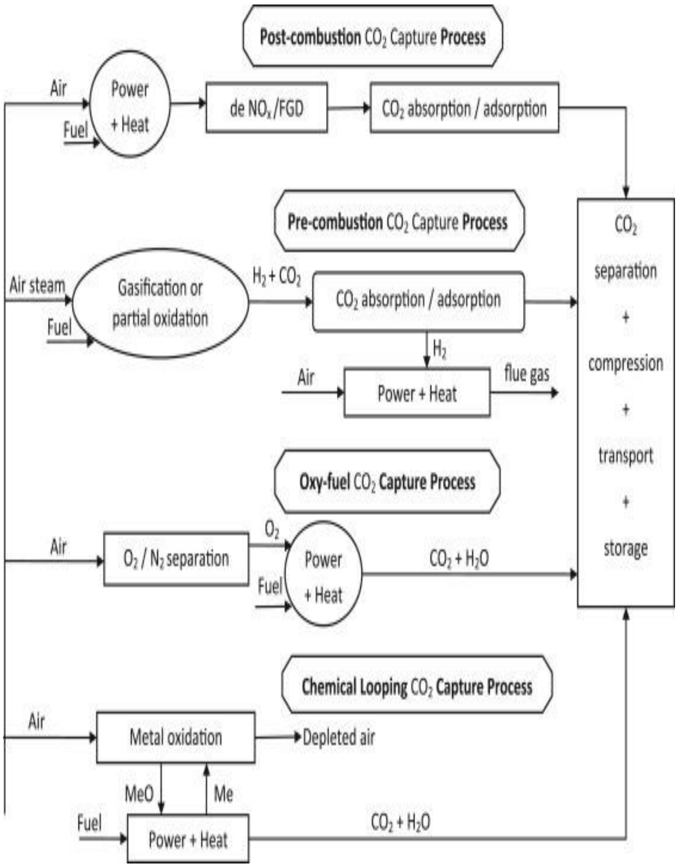

Fig. 1: Technology for CapturinG CO2

A. [14.] Post-combustion

After burning, CO2 is removed out of the flue gas using this procedure. The primary solution for retrofitting existing power plants is post-combustion technologies. [4.] With CO2 recovered at rates up to 800 t/day, the method has been demonstrated on a modest scale (Wall TF, 2002). The high parasitic load of post-combustion CO2 capture is the main obstacle, though. [15.] The energy penalty and related expenses for the capture unit to attain the concentration of CO2 (above 95.5%) needed for transport and storage are high because [10.] the CO2 level in combustion flue gas is typically fairly low (i.e. 7-14% for coal-fired and as low as 4% for gas-fired) (E. De Visser., [8.] 2008) (ICF, 2009) (A.A. Olajire, 2010). According to the U.S. National Energy Technology Laboratory, CO2 post-combustion capture would [8.] raise the price of producing power by 70% (L.C. Elwell et al., 2006) (According to a recent research, [4.] post-combustion in gas and coal-fired plants would result in increases in energy costs of 32% and 65%, respectively (M. Kanniche, et al., 2010) 16 [4.] large-scale integrated CCS projects have been identified as being in operation or being built, but only [4.] two of them use post-combustion technology (Global CCS Institute, 2012a).

B. Pre-combustion

The fuel, which is often [4.] coal or natural gas, is pre-treated in this process before combustion. For coal, the pretreatment entails a gasification process carried out in a gasifier at low oxygen level to create a syngas that is primarily free of other polluting gases and consists primarily of CO and H2 [9.] (Eq. 1). The syngas will next run through a water gas shift reaction, producing additional steam and H2 while converting CO gas to CO2 (Eq. 2):

$$\text{Coal} \quad \underline{\text{gasification}} \rightarrow \quad CO+H$$
$$CO+H2O \quad \underline{\text{gasification}} \rightarrow \quad H2+CO2$$
$$CH4+H2O \quad \underline{\text{gasification}} \rightarrow \quad CO+H2$$

[4.] The CO2 separation is made easier by the H2/CO2 fuel gas mixture's high CO2 concentration (>20%) (A.A.Olajire,2010) and common [6.] CO2 separation techniques are covered in Section 4. Following this, the H2 is burnt in the air, primarily releasing N2 and water vapor. It is possible to use [36.] pre-combustion capture in Integrated Gasification Combined Cycl e (IGCC) power plants that burn coal, although doing so will result in an efficiency loss of 7-8% (Wall TF, 2007) (Global CCS Institute, 2012b). A roadmap of IGCC technology advancements created by EPRI and the US DOE has the potential to increase IGCC efficiency to a level that is equal to or greater than that of the existing IGCC technology without capture (Global CCS Institute, 2012b). Since natural gas mostly consists of CH4, it can be transformed into syngas, which comprises [9.] H2 and CO (Eq 1). The water gas shift reaction (Eq. 2) can be used to increase the amount of H2, and the remaining steps are the same as those were previously outlined for coal (L.O. Nord et al.2 c009) performance's and [6.] cost studies on advanced combined cycle gas turbine facilities that burn natural gas and incorporate a pre-combustion CO2 capture system resulted in a CO2 capture efficiency of 80% and CO2 avoided costs of up to [8.] $29/t CO2 for an advanced design concept (Hoffman et al., 2009).

C. Oxygen fuel combustion

Oxyfuel combustion uses oxygen as fuel [35.] instead of air to burn. This lessens the amount of nitrogen in the exhaust stream that has an impact on the subsequent separation process. Natural procedure for separating waste. Another benefit of this technique is a significant reduction in thermal NOx (. When pure oxygen is used for combustion, CO2, water, particulates, and SO2 make up the majority of the exhaust gases. [6.] Traditional electrostatic precipitator and flue gas desulphurization techniques can be used to remove SO2 and particles, respectively. [4.] The residual gases, which have significant levels of CO2 (80–98% depending on the fuel used , can be compressed, transported, and stored. Although technically possible, this procedure uses a lot of oxygen that comes from an air separation unit that uses a lot of energy . As a result, there are significant financial costs, and the energy penalty may exceed 7% when [13.] compared to a plant without CCS . [13.] High SO2 levels in flue gas may also make corrosion issues in the system worse. There aren't any full-scale oxyfuel-fired projects between 1000 and 2000 MWth now in development, although [16.] a few small-scale commercial demonstration plants, such the 25 MWe plant, are and 250 MWe oxy-coal units, respectively, put forth by CS Energy and Vattenfall [29].

III. EXPERIMENTATION

By combining petroleum pitch carbon fiber (provided by [9.] Sinocarb CO. Ltd.) and phenolic resin (Durez 7716, provided by the Durez Corporation), large-scale honeycomb carbon fiber composites were created in our lab after [9.] a series of preparation steps, including molding, drying and curing, carbonisation, and activation. Earlier, a thorough explanation of the stages involved in fabricating an adsorbent, including their temperatures and times, was covered (Thiruvenkatachari et al., 2009a). The CSIRO lab designed and built the moulding unit for the manufacturing of these large-sized adsor- bents. For the large-scale carbon fiber composite, a burn-off amount of roughly 15-20% was not surpassed in order to preserve its structural stiffness. The enormous honeycomb carbon fiber that was created Figure illustrates a composite adsorbent. The surface morphology of the carbon fiber composite is depicted in Fig. 1(a) and the SEM picture (JEOL JSM6400F). 1(b).

The constructed adsorbent had a 123 mm diameter, and each composite was around 150 mm long. The carbon fiber composite employed for this study's channel configuration is depicted in Fig. 1(a). Flue gas is passed through a system of [9.] flow-through gas channels (267 channels, each 2.5 mm in diameter), and a system of channels (13, each 4 mm in diameter), which serve to [73.] indirectly heat and cool the system.

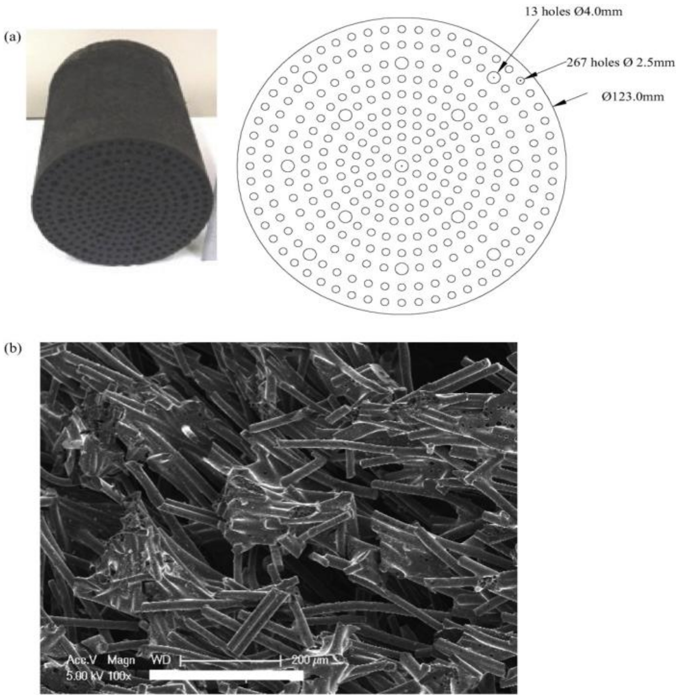

Fig. 2: A photograph of the carbon fiber composite that was created to capture CO2 and a microscopic view of the surface morphology are shown here (b)

Adsorbents were in the scene. Hot air and cold water were passed through stainless steel tubes with a 3.86 mm internal diameter and 13 channels in the adsorbents. Using a Tristar 3000 (Micromeritics, USA) device, the adsorbents were characterized to establish their CO2 adsorption capabilities, pore size, and pore volume. Using an ASAP 2020 (Micromeritics, USA) and the Density Function Theory, an isotherm analysis at 273 K was used to evaluate the samples' pore size distribution (PSD) (DFT).

A. *Set-up for an experiment*

The large-scale CO2 capture test equipment was created and developed to conduct adsorption and desorption tests using heat and vacuum. Fig. Diagrams [61.] can be seen in Fig. 2(a) and 2(b). The experimental setup is depicted in photographs in 2(b) (Thiruvenkatachari et al., 2009b).

The large-sized carbon fiber composite adsorbents were housed in two identical test columns that were each 2 m long and 203 mm in diameter. Inside the huge column was a stainless steel column with a 125 mm diameter. The area between the columns was vacuumed out and kept that way to serve as insulation. The manufactured adsorbents, which had a diameter of 123 mm, were inserted in the inner column and neatly arranged along the inner wall whole column length (Thiruvenkatachari et al., 2009b).

Thirteen tubes are positioned through the bigger channels in the complementary adsorbents to heat or cool the material with hot air up to 433 K or cold water down to 283 K. K-type thermocouple temperature probes were positioned [38.] at the top and bottom of the column (Thiruvenkatachari et al., 2009b).

The adsorbent material was heated to 403K using air heated in a furnace for thermal regeneration. The gases were removed from the column using a diaphragm vacuum pump. The computer software (created with Labview) was used to control the mass flow controllers (Sierra Instruments, USA), furnaces, and valves, and the data gathered were logged. The pneumatic valves could withstand gas temperatures up to 453 K and were operated by compressed air , [41.] A CO2 analyser (Madur Instruments, Spain) and an O2 analyser were used to measure the concentrations of CO2 and O2 in the adsorbent column's inlet and exit gases, respectively (PMA 10). A volume meter (DTA 750, Landis + Gyr, Australia) was used to determine how much gas was present. A mass flow meter was used to measure the flow (Sierra Instruments, USA).

B. *Experimental methodology*

In one column, the adsorbent mass was 4486 g. N2, O2, CO2, H2 O, and pollutants like SOx and NOx are commonly found in coal-fired power plants' flue gas. (Thiruvenkatachari et al., 2009b).

If necessary, a pre-treatment procedure can virtually completely remove H2O, SOx, and NOx. However, a simulated flue gas made up of CO2, O2, and N2 was used in this investigation. At 298 K, [9.] the inflow simulated flue gas contained a concentration of approximately 13% CO2 (partial pressure of 13 kPa), 5.5% O2, and the remaining N2. (Thiruvenkatachari et al., 2009b).

The mass flow controllers were used to mix air and pure CO2 in a set of ratios to create the simulated flue gas that was supplied to the system. Initially, simulated flue gas avoids the columns and goes directly to the sensors, where it is measured before the adsorption process begins (Thiruvenkatachari et al., 2009b).

The adsorption breakthrough experiments were conducted at 298K and at atmospheric pressure, with the simulated [37.] flue gas entering from the bottom and exiting from the top of the column holding the sorbents. Following the adsorption stage, pure CO2 product purge was also offered (Thiruvenkatachari et al., 2009b).

With a single or combined thermal and vacuum swing, hot air and/or vacuum were given to desorb the absorbed CO2 from the adsorbents. Regeneration of the adsorbent was done in thermal swing adsorption (TSA) [64.] by increasing the adsorbent bed's temperature up to 393 K (Thiruvenkatachari et al., 2009b).

No inert purge gas was employed to retrieve the desorbed gas from the column during thermal swing; it was simply permitted [64.] to leave from the top of the column by thermal expansion. The inlet of the adsorbent column was closed during vacuum swing adsorption (VSA), and the exit was attached to a vacuum pump. [44.]At a constant temperature of 303 K, the adsorbent bed was then evacuated to a pressure of 30 kPa. In a similar manner, purge gas was provided after the vacuum swing to return the column to atmospheric pressure. The adsorbent temperature was raised to 393 K with column intake and exit during the combined thermal and vacuum swing (TVSA) regeneration stage (Thiruvenkatachari et al., 2009b)

Closing the outlet, bringing the column's pressure down to 25 kPa, and then opening the outlet. Before beginning the process of adsorption once more, adsorbents were cooled to room temperature and He-purged. Helium was used in this research study to purge the adsorbed column before the start of the adsorption breakthrough test in order to ensure that the bed contains no residual CO2 or N2 from previous cycles or any pre-adsorbed gases. Helium shows virtually no adsorption on the microporous adsorbents at room temperature (Groszek, 1997). Similar procedures have been used.

IV. RESULTS AND DISCUSSION

A. *Adsorption equilibrium studies*

Our carbon composite's CO2 adsorption capacities at 298 K were around 2.65 and 0.73 mmol/g at 760 and 99 mmHg, respectively (considered as equivalent pressures for 13% CO2), which are about 67 and 103% greater than those of a commercial activated carbon as shown in Fig. 3(a). The micropore size distribution (MPSD) of a solid adsorbent is directly correlated with its capacity to adsorb CO2 because, at 298 K and 760 mmHg, CO2 molecules are primarily adsorbed in small micropores (Konstantakou et al., 2007). A statistical and representative phrase used to describe individual pores is the pore size distribution (PSD).

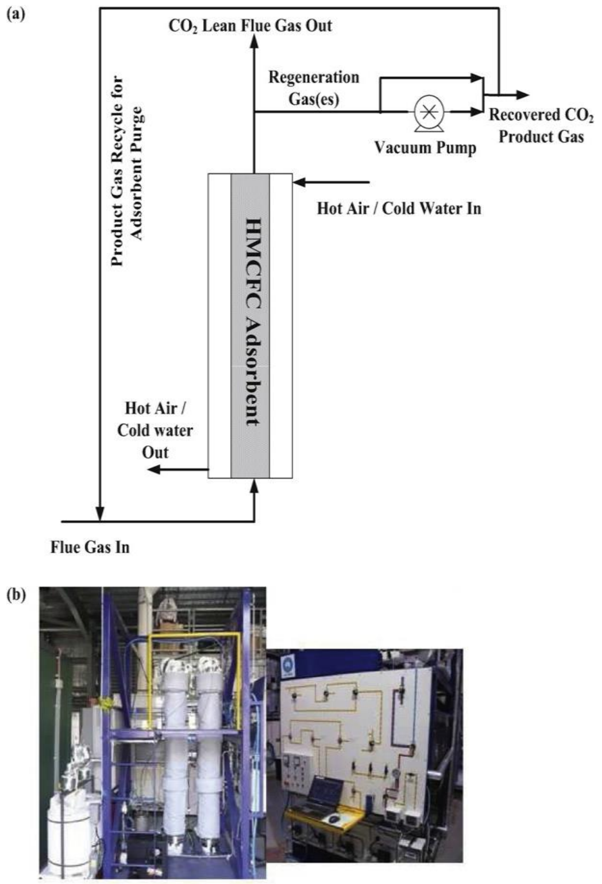

Fig. 3: Diagram and image of a large-scale CO2 adsorption unit with heat and vacuum swing regeneration are shown in (a) and (b), respectively

based on the way that a porous material adsorbs the behavior of the probe molecules (Konstantakou et al., 2007). The CO2 mass transport through the porous solid is represented by the PSD derived from equilibrium isotherms of CO2. Consequently, the PSD is a related concept. The following explanations explain why using CO2 adsorption isotherms to determine the PSD of the adsorbent is most suitable:

This study addresses CO2 capture.

- CO2 adsorption covers pore at 273 K and ambient pressure.

To a certain extent, the intended average pore size might be controlled using carbon fiber and fabrication circumstances to fit the preferred capture of the target gas [9.] (Thiruvenkatachari et al., 2009a,b).

The ability of these carbon fiber composites to absorb CO2 The recently discovered metal organic framework (MOF) family of adsorbents (Mohanty et al., 2011) similarly shown higher CO2 adsorption capabilities under ambient circumstances, as shown in Table 1, which were nearly twice that of commercial activated carbon (Thiruvenkatachari et al., 2009a). Sizes up to 9A Fig.4 depicts CO2 and

N2 adsorption isotherms in our car-bon composites.

Table 1: ***Comparing the CO2 adsorption capabilities of MOF class adsorbents and carbon fiber composites***

a The first maximum pore size determined using PSD.

- At coal fired PCC settings (10-15% and 25 °C), micropores smaller than 6 A are more significant to CO2 collection (Martin et al., 2010).

Figure 1 illustrates this. [54.] In comparison to commercial activated carbon (GC C-30 pelletized activated carbon), carbon fiber composite demonstrates significantly higher micropore space, especially for pores spanning from 4 to 6 A in pore width, [54.]which is important for CO2 extraction from flue gas.

Typically, in disordered and amorphous materials, physical activation with CO2 occurs first.

Carbon components and flaws, opening small pore spaces, widening pore spaces, and eventually, with further activation, decreasing the population of small pores. Our past research has shown that with the appropriate choice of at various temperatures, bon composite (273, 298 and 323 K). The initial slopes of the CO2 isotherms were higher than those of the N2 isotherm, as was to be expected. How well the adsorbent separates CO2 from its combination with N2 is indicated by the ratio of the CO2 and N2 adsorption isotherms at the Henry's Law region. The ratio was discovered to be 15.4 at 298 K, which satisfies the condition for efficient gas separation (Donald Carruthers et al., 2012; Yang, 2008). Due to the [24.] fact that the isosteric heat of adsorption depends on pressure The heat of adsorption, which is equal to [72.] the isosteric heat at zero loading, is a more pertinent word to describe CO2 capture at pulverized coal burned PCC settings due to its lower concentration, which decreases[18.] with an[18.] increase in the adsorbed amount.

Bet Surface Area (m^2/g)	Pore Volume)cm^3/g)	Pore width (from DFT with CO2(nm)	CO2 uptake @ 25°C, 1 bar	
			Mmol/g	Wt%
851	0.434	0.55-0.62	1.9	8.3
1061-1312	0.31-0.78	0.53-0.57^a	2.51-3.1	11.1-13.67
988	0.55	0.57^a	1.518	6.6

Table 1: CO2 adsorption isotherms and micropore size distributions in our carbon composite and a commercially available activated carbon (a) (b)

In comparison to N2. Clausius-Clapeyron equation calculations showed that the heat of CO2 adsorption on our carbon fiber composite was 32 [50.] kJ/mol at zero loading, which is higher than the heat of adsorption on typical activated carbons, demonstrating that our composite has well-developed narrow micropores and a higher CO2 adsorption capacity. Although the CO2 heat of adsorption of the carbon fiber composite is greater than that of activated carbon adsorbents (12–30 kJ/mol) [39.] (Guo et al., 2006; Liu et al., 2012; Xing et al., 2012), it is significantly less when compared to other adsorbents like zeolites (22–50.5 kJ/mol) (Ahn et al., 2004; (2010); Li et al. (2011)). The conditions for adsorbent renewal must also be determined by the [11.]heat of adsorption.

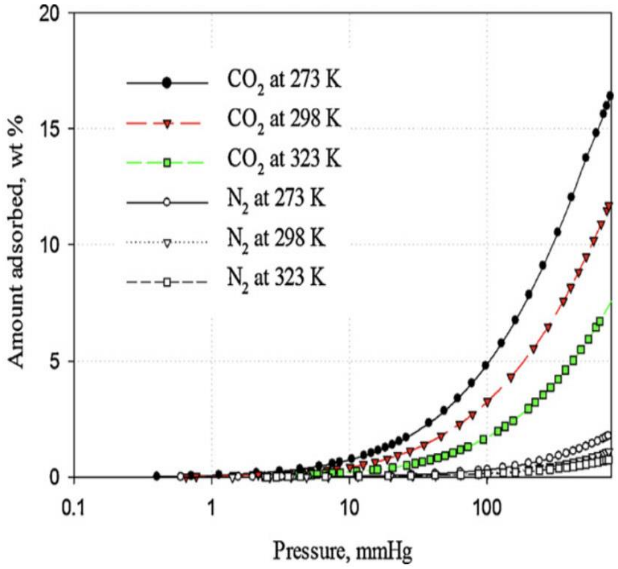

Fig. 4: [11.]CO2 and N2 adsorption isotherms in our carbon composite at three different temperatures (273, 298 and 323 K)

High temperature during regeneration is necessary for a higher heat of adsorption. The results from this study implies that the highest temperature needed for a carbon fiber composite to regenerate completely is 398 K, as will be covered in the next sections of this article. In Australia, pulverized coal-fired power plants typically have flue gas temperatures between 393 and 453 K. (Feron, 2012; Lee and Sircar, 2008). These adsorbents might be thermally regenerated using the waste heat from the exhaust flue gas.

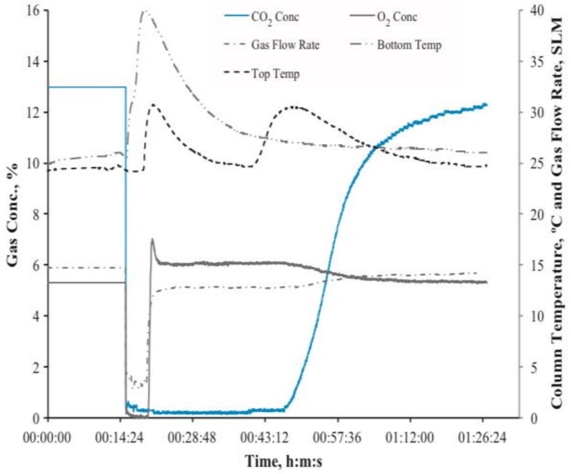

Fig. 5: Temperature profile and typical CO2 adsorption breakthrough profile in the adsorption kinetic investigation.

B. New study on dynamic CO2 adsorption

Fig. The whole dynamic adsorption breakthrough profile is shown in Figure 5. After initial regeneration of the sorbents, when the [46.] simulated flue gas (at 298 K) with a constant CO2 concentration of [12.]13 vol% (partial pressure 13 kPa) enters the adsorption column, the sorbents start to capture over 98% of CO2, and the exit CO2 concentration declines to less than 0.2% (Thiruvenkatachari et al., 2009b). The outlet CO2 concentration starts to rise as the break-through time approaches, finally reaching the point where the column is totally saturated and no longer able to capture any more CO2 (at that concentration). The output CO2 concentration is now equal to the inflow concentration. (Thiruvenkatachari et al., 2009b).

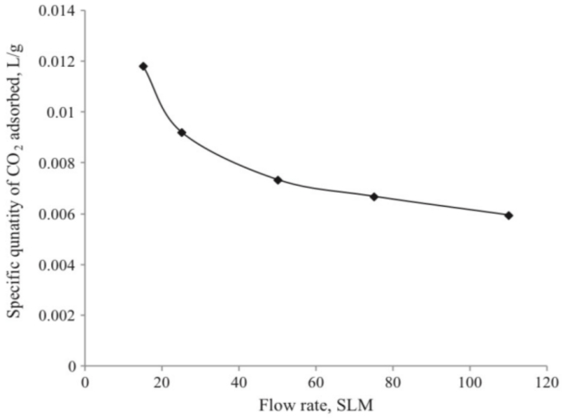

Fig. 6: CO2 uptake till breakthrough at different flow rates.

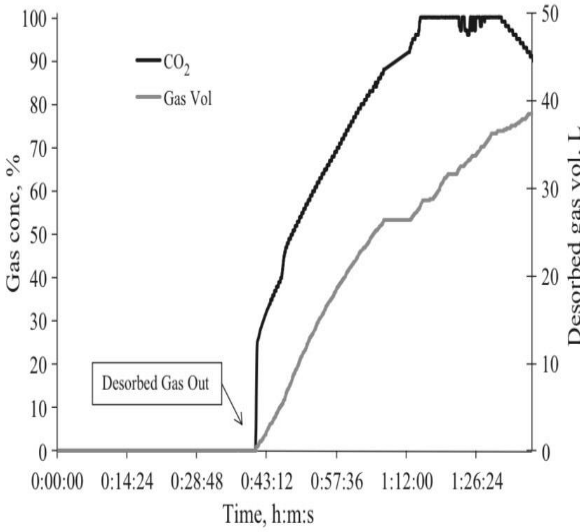

Fig. 7: Temperature-induced CO2 concentration

The material preferentially adsorbs CO2 when flue gas enters the column, but it also invariably adsorbs other gases like O2 (and nitrogen) that are present in the flue gas. Fig. shows it clearly. Compared to CO2, the O2 breakthrough occurs considerably sooner. At this stage, O2 and N2 make up the majority of the output stream, and the flow rate rises and approaches the inlet flow rate of 15 square linear meter. The concentration of O2 overshot its inflow concentration as adsorption progressed. During competitive adsorption in a multicomponent gas stream, the desorption of a comparatively weak adsorbate causes this effect (Moon and Shim, 2006; Thiruvenkatachari et al., 2009b). It demonstrates the presence of the highly adsorbing species CO2.

The carbon fiber composite adsorbent is more effectively absorbed as compared to O2. In prior investigations, a similar impact was observed during the adsorp-tion of methane and carbon dioxide gas mixtures (Moon and Shim, 2006; Thiruvenkatachari et al., 2009b). It was discovered that the CO2 capture capacity measured from the breakthrough experiments (under dynamic conditions) was approximately 0.02 g/g carbon, which is marginally less than the value (0.03 g/g) obtained from the CO2 adsorption isotherm experiments (equilibrium condition), corresponding to 13% CO2. The heat from CO2, N2, and O2 adsorption causes the adsorbent temperature in the column to be significantly greater than the starting temperature prior to the CO2 breakthrough period. Co-adsorption of N2 and O2 would additionally decrease the CO2 capture capacity.

Figure 5 illustrates this. It was discovered that the column's highest temperature had two humps. The heat produced by N2 and O2 adsorption causes the first hump, and the heat produced by CO2 adsorption, which has moved [17.] from the bottom of the column to the top, causes the second. The CO2 in the gas stream (exiting the column) is first detected at the crest of this hump, which is also the location of breakthrough (Thiruvenkatachari et al., 2009b) . [43.] As can be observed from the bottom temperature profile, the bottom of the column, which has already reached exhaustion, has been cooled by the inlet gas stream. Thiruvenkatachari et al., 2009b)

Different simulated flue gas flow rates were fed into the column, and the rate of CO2 adsorption over time was measured and studied. Figure 6 illustrates the precise amounts of CO2 adsorbed (litres of CO2 per gram of adsorbent) during the breakthrough time. The breakthrough time or the amounts of CO2 adsorbed did not decrease linearly with an increase in flow rate. Similar profiles were seen in earlier research as well (Jee et al., 2004; Mohan et al., 2009). The two main mass transport processes in the column are viscous flow through the flue gas channels and Knudsen diffusion through pore spaces. When the flow rate is modest, the mass transfer is dominated by the diffusion process. However the size of the flue gas channels is significantly larger than that of the Knudsen diffusion regime (meso/macropores), which results in an early breakthrough time and less CO2 collection as the feed flow rate rises (Bae and Do, 2005).

C. Thermal regeneration

The desorption of adsorbates occurs as the temperature of the adsorbent is raised. Following the CO2 breakthrough period, the adsorption process is halted, and the carbon fiber composite adsorbents are then heated to remove the adsorbed CO2 (and other gases like O2 and N2) from the material. By analyzing the desorbed gas quality (the CO2 concentration) and amount of CO2 able to be removed, the performance of the desorption process was was successful in achieving. However, fewer than 10 L of pure CO2 (or more than 95%) was recovered during thermal regeneration alone out of the 53 L of CO2 that the material had absorbed during the adsorption process (Thiruvenkatachari et al., 2009b).

The desorption temperature is one of the elements impacting the quantity and quality of desorption gas (in terms of CO2 concentration). The amount of gas that can be extracted by heating the adsorbent to different temperatures is shown in Table 2 together with the highest CO2 [23.] ``content in the desorbed gas. (Thiruvenkatachari et al., 2009b) The concentration of CO2 gas increased as the desorption temperature rose to as high as 398 K. As the desorption temperature climbed, so did the amount of gas extracted. The partial pressure of the CO2 [68.]at the end of this phase of regeneration is equivalent to air pressure, therefore it was obvious that no matter what the temperature for regeneration, it was not possible to remove all the gases from the adsorbent material by applying heat alone. Thiruvenkatachari et al., 2009b)

Average desorption temperature (K)	Max CO2 concentration (%)	Desorbed Gas Voume (L)
333	42	8
358	59	20
398	100	39

Table 2: Performance of thermal desorption at various desorption temperatures.

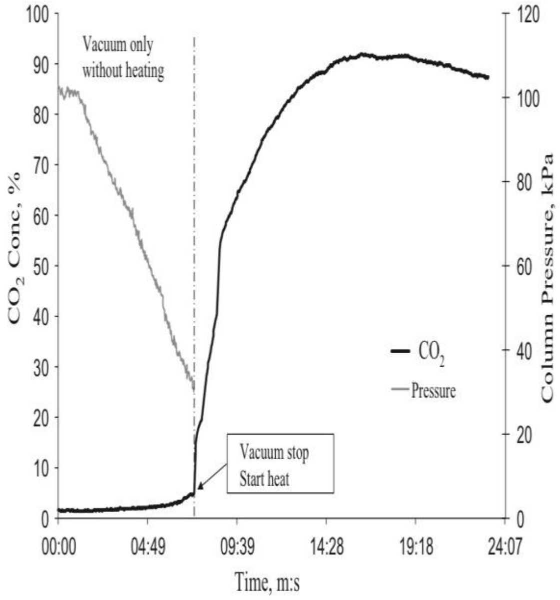

Fig. 8: CO2 concentration and column pressure when applying heat and throughout individual vacuum swing desorption processes

D. *Regeneration in a vacuum*

Instead of applying heat immediately after the adsorption process, vacuum was used during the vacuum swing desorption process, [40.] and the concentration of CO2 in the desorbed gas was observed. Figure 1 illustrates this point. When only vacuum was utilized to remove the adsorbed CO2, the CO2 concentration in the desorbed gas was very low. Up to roughly 30 kPa of vacuum, a CO2 concentration of about 4.5% was observed. The final vacuum level must be carefully evaluated because it will significantly [18.] affect the process's operating costs (Shen et al., 2012). Because the concentration of desorbed CO2 did not significantly rise with In this study, it was not necessary to apply vacuum down to 30 kPa, further lowering the vacuum pressure. Due to the strong interaction between CO2 and the adsorbent, a single step vacuum regeneration was insufficient to properly remove the CO2 adsorbed. Similar results were seen on carbon and amine-grafted mesoporous silica sorbents [47.](Serna-Guerrero et al., 2010; Dutcher et al., 2011). Applying vacuum, on the other hand, was more effective in removing O2 (and to a lesser extent N2) from the sorbent material. Moreover, Fig. 8 also shows that the adsorbed CO2 must be heated in order to be released from the substrate. [52.] It is evident that the concentration of CO2 starts to rise as soon as heat is applied. This shows that an efficient desorption process would involve a vacuum and thermal process working together.

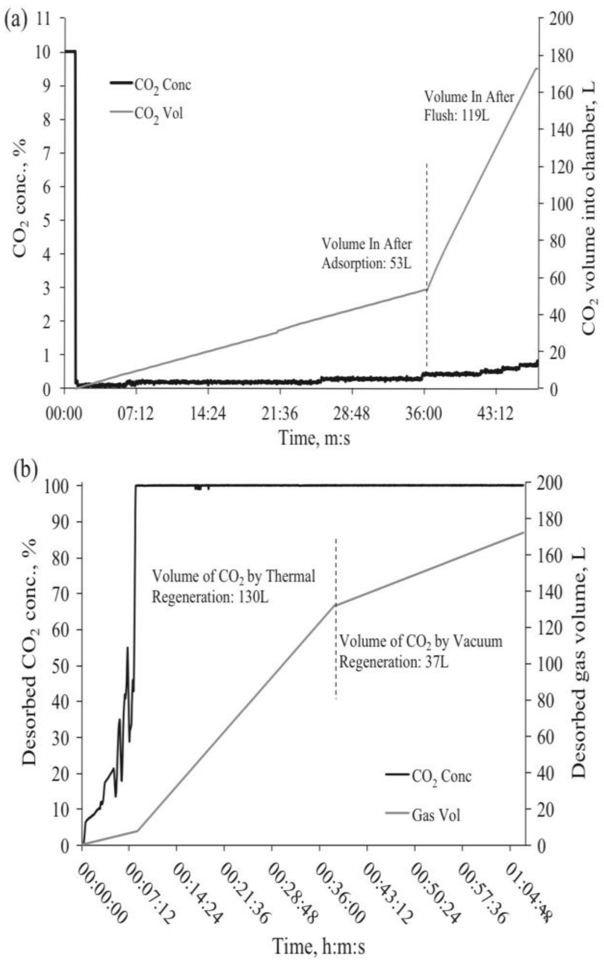

Fig. 9: Performance of the combined thermal and vacuum swing desorption system (mass of adsorbent: 4486 g) (a) CO2 concentration during adsorption and flushing (b) CO2 concentration of the desorbed gas during thermal and vacuum regeneration

Another effort used flushing with a pure CO2 product displaced the weakly adsorbed N2 component (as well as O2) that was present in the adsorbents and in the empty volume when it was added [17.] at the end of the adsorption process. The temperature of the bed rose as a result of the CO2 purge stream, and this temperature profile (measured using sensors [67.] at the top and bottom of the bed) was used as a gauge to gauge how much CO2 was being purge and when the bed was becoming saturated. The bed needed about 0.0354 L of pure CO2 purge/g of adsorbent to reach saturation. During the purge step, [60.] the CO2 concentration at the column exit was less than 2%, and N2 and O2 were displaced from the bed. Any additional purges added caused the outlet's CO2 content rapidly rising. After the purge, evacuation was conducted, and it was discovered that although the CO2 concentration was completely desorbed throughout, fewer than 40% of the CO2 that had been introduced could be retrieved. During this vacuum step, column pressure was reduced to 25 kPa.

E. Combined Thermal and Vacuum Regeneration

After a number of tests with different CO2 flushing quantities, it was determined that particular CO2 quantity in order to minimize the capture cost, excess purge amount must be avoided (Zhang, 2008). Very high desorption gas quality and good recovery were attained with time, h:m:s of 0.0265 L/g. Fig. The outlet CO2 concentration was extremely low (less than 0.3% during adsorption and less than 0.5% during flushing) as can be seen in 9a, which also shows the CO2 concentration profile and the volume of CO2 introduced during adsorption and flushing (Zhang, 2008). Adding a brief cooling step to bring the bed temperature to room temperature after the adsorption step was able to further reduce the outlet CO2 concentration during pure CO2 flushing (Zhang, 2008). The CO2 concentration quickly reached 100% and remained high throughout the remainder of the thermal and vacuum desorption steps when the adsorbent was heated up to 398 K during thermal regeneration, with the exception of the first phase when the desorbed gas exited the column, which had a CO2 concentration less than 50%. (Fig. 9b). Over 95% of CO2 was recovered (Zhang, 2008).

The addition of a brief vacuum step during the last stages of bed saturation considerably reduced the amount of pure CO2 flushing necessary to replace N2 and O2 (Zhang, 2008). After 102 L of pure CO2 flushing, the residual N2 and O2 in the bed were removed using vacuum (up to 75 kPa). When the bed was further evacuated, the level of CO2 in the air shot up quickly in the plug. The top bed temperature rapidly increased as the pure CO2 being extracted traveled through the top section of the column and was re-adsorbed. Following the evacuation phase, CO2 was recovered via thermal and vacuum regeneration. The recovery rate was over 97% and the [60.]CO2 concentration in the outflow reached 100% under this optimal working condition. Fig. In the optimized combined heat and vacuum swing regeneration process, Figure 10 depicts the CO2 concentration and gas volumes during the adsorption, flush, and regeneration stages.

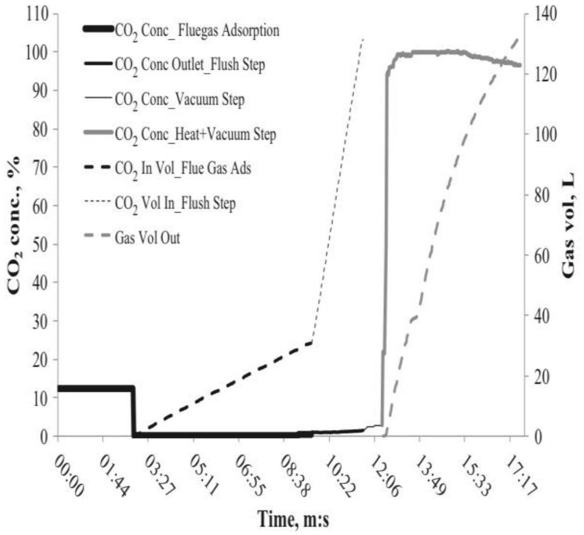

Fig 10: Performance of a heat and vacuum swing regeneration technique that has been optimized (mass of adsorbent: 4486 g)

This study has shown that combining heat and vacuum regeneration increases desorption efficiency compared to using either thermal or vacuum regeneration alone (Table 3). Greater CO2 recovery and concentration of recovered CO2, shorter regeneration times, and minimal heat and vacuum pressure requirements are some benefits of a combined system (Boger et al., 1997; Plaza et al., 2010; Wang et al., 2012) [22.]. Previous investigations on activated carbon adsorbents also showed these advantages of a combined thermal and vacuum regeneration approach over separate processes [20.] (Boger et al., 1997; Plaza et al., 2010; Wang et al., 2012).

The basic steps of the combined heat and vacuum swing regeneration process for a single bed system are shown in Figure 11. There are four key steps in the process design. In Step II, preferential CO2 adsorption from the flue gas occurs; once the breakthrough point is reached, a portion of the desorbed product CO2 obtained from the thermal and vacuum swing in Step IV is used in Step III's purge step, which enables additional CO2 adsorption and removes N2 and oxygen from the adsorbents. Overall, this purge stage allows for more concentrated CO2 gas to be recovered in the subsequent regeneration step (Step IV). Following the extraction of the adsorbed gases from the column, the adsorbents are cooled to room temperature and ready (Stage I) for the restart of the CO2 adsorption step (Boger et al., 1997; Plaza et al., 2010; Wang et al., 2012).

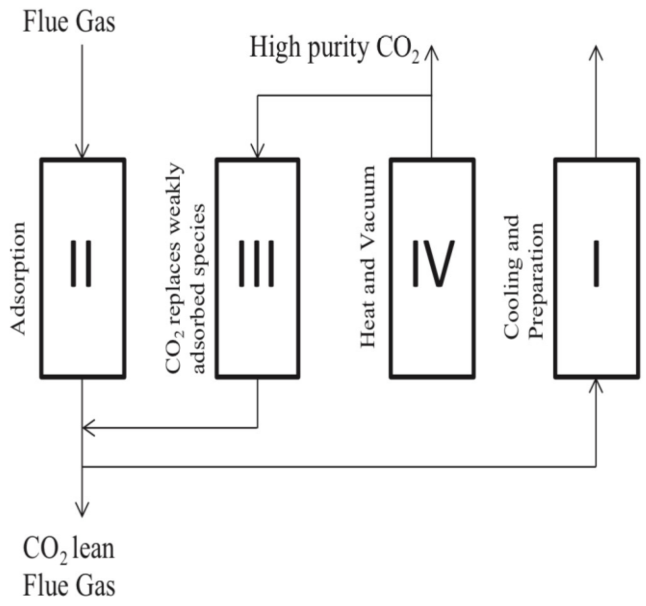

Fig. 11: Combining CO2 capture with thermal and vacuum swing regeneration is the process order

Depending on the kind, the typical composition of flue gases in Australia 10–13% CO2, 75% N2, 4% O2, and 6–12% of the total amount of coal consumed H O, 200–800 ppm SO2, and 350–700 ppm NO2 (Ho et al., 2009; 2 (2006) Sass et al. The exhaust flue gas's temperature is typically between 393 and 453 K. The [2.] honeycomb monolithic carbon fiber composite adsorbent reported in this article is being created primarily for removing CO2 from flue gas produced by stationary fossil fuel-fired plants, including coal-fired power plants. Future applications are predicted to include at [2.] least two monolithic carbon fiber composite vessels in a CO2 capture system,[2.] as an example; however, the precise configuration and quantity of vessels will depend on a variety of factors. Elements include the power plant's parameters and the amount of processed gas. The three-vessel system would enable switching of the process [2.]between the vessels, with adsorption taking place in one, desorption in another, and the third in a preparation stage for adsorption in the cycle.

Nearly all suggested CO2 sorption processes call for flue gas pre-treatment to remove trace SOx, NOx, moisture, and particulates, as well as cooling the flue gas to ambient temperature (Feron and Paterson, 2011; Ho et al., 2009; Pires et al., 2011; Sass et al., 2005; Zhang et al., 2009)[14.]. The typical operating temperature for the solvent-based absorption process employing monoethanolamine (MEA) is 313 K, and the presence of of oxygen and contaminants in the flue gas of acid gas [24.](Ho et al., 2009; Sass et al., 2005). The operational capacity to adsorb CO2 from flue gas could potentially be affected[11.] by the presence of moisture, SOx, and NOx. Physical adsorption processes using carbon adsorbents are typically run at 298 K or above (adsorption capacity decreases with increase in temperature). However, in this situation, Sjostrom and Krutka (2010) and Sjostrom et al. (2011) compared a variety of adsorbent materials and discovered that [11.] carbon-based adsorbents demonstrated superior cyclic (capture and regeneration) stability and showed [34.]little to no effect from the presence of trace flue gas constituents. Carbon adsorbents are more water-tolerant than zeolites (D'Alessandro et al., 2010; Radosz et al. (2008)[30.] , Xu et al. (2011), Pires et al. (2011), and others. It was also noted that during the regeneration studies with repeated heating and cooling, the carbon fiber composite adsorbent was unaffected by water from moisture condensation. We are doing a study to determine the impact of SOx, NOx, moisture, and particles on CO2 capture performance by testing carbon fiber composites with actual flue gas from a power plant. For application in high dust environments, carbon fiber composites with parallel flow through channels would be preferable to the[2.] monolithic catalysts currently used in flue gas selective catalytic reduction (SCR) De-NOx processes in pulverized coal fired power plants (Forzatti, 2001; Su and Agnew, 2006).

Regeneration Method	Max CO2 purity (%)	CO2 recovery (%)
Thermal regeneration	100	50
Vacuum regeneration	5	10
Combined thermal and vacuum regeneration with CO2 flush	100	95
Optimised thermal and vacuum regeneration with minimum CO2 flush	100	97

Table 3: Purity of CO2 and various regeneration techniques

There have proven that this sort of honeycomb monolith is capable of handling up to 30 g/Nm3 dust in the SCR process (Su and Agnew, 2006).

However, there are certain practical challenges with adsorbents in establishing efficient heat exchange in the heating and cooling cycles of the capture and regeneration process (Mulgundmath et al., 2012; Wang et al., 2012) [20.] In the current work, a series of 13.5 mm stainless steel tubes were inserted along the length of the carbon fiber composite adsorbents and used to circulate warm air and cold water to heat and cool the adsorbents, respectively. The way things were set up, heat transfer wasn't working as well as it should have. It took 20 to 30 minutes to heat the adsorbents from 303 to 398 K during thermal regeneration (Mulgundmath et al., 2012; Wang et al., 2012). Due to the small heat transfer area and heat loss via the column shell, the temperature of hot air is 423 K. [55.] Prior to the start of the adsorption cycle, adsorbents were cooled to 298 K using chilled water at 283 K after thermal regeneration [20.](Mulgundmath et al., 2012; Wang et al., 2012). Several changes are being thought about to improve the heat transfer. Taking the size of the heating and cooling channels as an illustration The diameter of each cylindrical adsorbent has been increased to 13 mm. Performance in heat transfer has not yet been evaluated [48.]12(Mulgundmath et al., 2012; Wang et al., 2012)

(Sjostrom and Krutka,2010) assessed the energy consumption of different carbon-based adsorbents used in CO2 capture with thermal regeneration and compared it to the benchmark MEA absorbent, which had a theoretical [12.] energy consumption of 4.5 MJ/kg CO2. They stated that the hypothetical energy requirements for carbon adsorbents ranged from 7.2 to 17.2 MJ/kg CO2. Zeolite adsorbents ranged from 3.4 to 35.2 MJ/kg CO2 under the same comparison. Thermal and vacuum regeneration of carbon nanotube adsorbents with strongly loaded amine was reported to need 2.522 MJ/kg CO2 (Su et al., 2011). The anticipated cost of recovering CO2.

Thermal regeneration cost $27/tonne (after compression - pipeline ready) and vacuum regeneration cost $44/tons for activated carbon adsorbents, respectively, according to Radosz et al. (2008) (after compression). This can be contrasted with the benchmark amine process employing MEA, which has an average price of $58/tons (ranges from $40 to $74/tonne) (Ho et al., 2009; IEA, 2011; Radosz et al., 2008). The results from CO2 capture using actual[57.] flue gas from the power station with and without pre-treatment would be needed to determine the overall energy requirement more precisely. An evaluation of the energy requirements for CO2 capture for carbon fiber composite adsorbents using simulated flue gas for the CO2 capture with thermal and vacuum regeneration has been attempted.

V. CONCLUSIONS

There have been successful large-scale investigations on CO2 capture utilizing honeycomb carbon fiber composites. The following are some of the study's main conclusions:

- The large-sized carbon fiber composite in the shape of a honeycomb (HMCFC) adsorbents displayed extremely strong CO2 adsorption on average.11.9% capacity (at 293 K and 1 atm) (Su et al., 2011). The capacity for adsorption compared to commercial activity, this HMCFC was found to be twice as much comparable to the MOF class of adsorbents and vated carbon (Su et al., 2011). The profile of pore sizes revealed that a favorable region of when compared to raw activated carbon fiber, the produced composite's 2 pore space was also larger. It suggests that the carbon fiber composite has a higher adsorption capability (Su et al., 2011).
- Over 98% of CO2 was successfully captured during the adsorption breakthrough investigation, and it was adsorbed more readily than other gases in the exhaust gas(Su et al., 2011). The saturation and adsorption of adsorbent material are clearly indicated by the temperature profile. A faster rate of flue gas flow led to a shorter adsorption breakthrough time. At higher adsorption temperatures, the adsorption capacity and breakthrough time were also reduced (Su et al., 2011).
- Thermal desorption was insufficient to completely eliminate the adsorbent substance, absorbed gas. But the quantity of gas removed rose as desorption increased in temperature. In a similar vein, vacuum alone was ineffective in removing adsorbed CO from the substance. Using heat in addition to vacuuming was better in removing CO2 from the atmosphere. This proves that Vacuum plus thermal desorption combination would be a more effective efficient CO2 collecting method (Su et al., 2011).
- Implementing pure CO2 flushing following adsorption's ability to replace the N2 and O2 that are weakly adsorbed and exist in the adsorbents and void volume (Su et al., 2011). [65.] However, it was critical to optimize the amount of CO2 needed to achieve high CO2 product purity and high recovery (and would also result in lowering the capture cost). Less than 40% of the pure CO2 that was flushed to completely saturate the adsorbent bed and remove all of the N2 and O2 was recovered (Su et al., 2011).
- The quantity of CO2 needed for flushing was lowered to with systematic optimization and the addition of a brief vacuum step (up to 50kPa) at the conclusion of flushing (Su et al., 2011) 0.0227 L/g. Through this method, the desorption gas showed a 100% CO2 content with a recovery rate of over 97% from the input flue gas.
- Because heat transport was inefficient in the current configuration, heating and cooling times were lengthy. To increase heat transfer efficiency, more design changes to the column and composite material are needed (Su et al., 2011).

ACKNOWLEDGMENTS

This is to especially appreciate our Research Department head assistance at Innostrukt Co.

REFERENCES

[1.] Ahn, H., Moon, J.-H., Hyun, S.-H., Lee, C.-H., 2004. Diffusion mechanism of carbon dioxide in zeolite 4A and CaX pellets. Adsorption 10, 111–128.

[2.] An, H., Feng, B., Su, S., 2009. CO2 capture capacities of activated carbon fibre-phenolic resin composites. Carbon 47, 2396–2405.

[3.] An, H., Feng, B., Su, S., 2011. CO2 capture by electrothermal swing adsorption with activated carbon fibre materials. International Journal of Greenhouse Gas Con- trol 5, 16–25.

[4.] Audus, H., 1997. Greenhouse gas mitigation technology: an overview of the CO2 capture and sequestration studies and further activities of the IEA greenhouse gas R&D programme. Energy 22, 217–221.

[5.] Bae, J.-S., Do, D.D., 2005. Permeability of subcritical hydrocarbons in activated car- bon. AIChE Journal 51, 487–501.

[6.] Boger, T., Salden, A., Eigenberger, G., 1997. A combined vacuum and temperature swing adsorption process for the recovery of amine from foundry air. Chemical Engineering and Processing: Process Intensification 36, 231–241.

[7.] 1997. A novel process and material for the separation of carbon dioxide and hydrogen sulfide gas mixtures. Carbon 35, 1279–1294.

[8.] Burchell, T.D., Omatete, O.O., Gallego, N.C., Baker, F.S., 2005. Use of carbon fibre com- posite molecular sieves for air separation. Adsorption Science and Technology 23, 175–194.

[9.] D’Alessandro, D.M., Smit, B., Long, J.R., 2010. Carbon dioxide capture: prospects for new materials. Angewandte Chemie International Edition 49, 6058–6082. DCCEE, 2012. Quarterly Update of Australia’s National Greenhouse Gas Inventory: December 2011. The Department of Climate Change and Energy Efficiency, Australia. Demessence, A., D’Alessandro, D.M., Foo, M.L., Long, J.R., 2009. Strong CO2 binding in a water-stable, triazolate-bridged metal–organic framework functional- ized with ethylenediamine. Journal of the American Chemical Society 131, 8784–8786.

[10.] Donald Carruthers, J., Petruska, M.A., Sturm, E.A., Wilson, S.M., 2012. Molecular sieve carbons for CO2 capture. Microporous and Mesoporous Materials 154, 62–67.

[11.] Drage, T.C., Smith, K.M., Pevida, C., Arenillas, A., Snape, C.E., 2009. Development of adsorbent technologies for post-combustion CO_2 capture. Energy Procedia 1, 881–884.

[12.] Dunne, J.A., Rao, M., Sircar, S., Gorte, R.J., Myers, A.L., 1996. Calorimetric heats of adsorption and adsorption isotherms. 2. O_2 , N_2 , Ar, CO_2 , CH_4 , C_2 H_6 , and SF_6 on NaX, H-ZSM-5, and Na-ZSM-5 zeolites. Langmuir 12, 5896–5904.

[13.] Dutcher, B., Adidharma, H., Radosz, M., 2011. Carbon filter process for flue-gas car- bon capture on carbonaceous sorbents: steam-aided vacuum swing adsorption option. Industrial and Engineering Chemistry Research 50, 9696–9703.

[14.] Feron, P., Paterson, L., 2011. Reducing the Costs of CO_2 Capture and Storage (CCS). CSIRO Energy Technology, NSW.

[15.] Feron, P.H.M., 2012. Assessing Post-Combustion Capture for Coal-Fired Power Station in Asia-Pacific Partnership Countries. CSIRO, Australia.

[16.] Feron, P.H.M., Hendriks, C.A., 2005. CO_2 capture process principles and costs. Oil and Gas Science and Technology – Revue de l’Institut Français du Petrole 60, 451–459.

[17.] Forzatti, P., 2001. Present status and perspectives in de-NOx SCR catalysis. Applied Catalysis A: General 222, 221–236.

[18.] Gray, M.L., Champagne, K.J., Fauth, D., Baltrus, J.P., Pennline, H., 2008. Performance of immobilized tertiary amine solid sorbents for the capture of carbon dioxide. International Journal of Greenhouse Gas Control 2, 3–8.

[19.] Groszek, A.J., 1997. Irreversible and reversible adsorption of some heavy transi- tion metals on graphitic carbons from dilute aqueous solutions. Carbon 35, 1329–1337.

[20.] Guo, B., Chang, L., Xie, K., 2006. Adsorption of carbon dioxide on activated carbon. Journal of Natural Gas Chemistry 15, 223–229.

[21.] Haq, N., Ruthven, D.M., 1986. A chromatographic study of sorption and diffusion in 5A zeolite. Journal of Colloid and Interface Science 112, 164–169.

[22.] Ho, M.T., Allinson, G.W., Wiley, D.E., 2009. Factors affecting the cost of capture for Australian lignite coal fired power plants. Energy Procedia 1, 763–770.

[23.] IEA, 2008. Energy Technology Perspectives 2008: Scenarios & Strategies to 2050. OECD/IEA, France.

[24.] IEA, 2011. Cost and Performance of Carbon Dioxide Capture from Power Generation. Cedex, France.

[25.] IPCC, 2005. Special report on carbon capture and storage. In: Metz, B., et al. (Eds.), Working Group III of the Intergovernmental Panel on Climate Change. IPCC, Cambridge, UK, New York.

[26.] Jee, J.-G., Lee, S.-J., Lee, C.-H., 2004. Comparison of the adsorption dynamics of air on zeolite 5A and carbon molecular sieve beds. Korean Journal of Chemical Engineering 21, 1183–1192.

[27.] Keskin, S., vanHeest, T.M., Sholl, D.S., 2010. Can metal–organic framework materials play a useful role in large-scale carbon dioxide separations? ChemSusChem 3, 879–891.

[28.] Kikkinides, E.S., Yang, R.T., Cho, S.H., 1993. Concentration and recovery of carbon dioxide from flue gas by pressure swing adsorption. Industrial and Engineering Chemistry Research 32, 2714–2720.

[29.] Kittel, J., Idem, R., Gelowitz, D., Tontiwachwuthikul, P., Parrain, G., Bonneau, A., 2009. Corrosion in MEA units for CO_2 capture: pilot plant studies. Energy Procedia 1, 791–797.

[30.] Konstantakou, M., Samios, S., Steriotis, T.A., Kainourgiakis, M., Papadopoulos, G.K., Kikkinides, E.S., Stubos, A.K., 2007. Determination of pore size distribution in microporous carbons based on CO_2 and H_2 sorption data. In: Llewellyn, P.L., Rodríguez-Reinoso, F.J.R., Seaton, N. (Eds.), Studies in Surface Science and Catal- ysis. Elsevier, Aix-en-Provence, France, pp. 543–550.

[31.] Lee, K.B., Sircar, S., 2008. Removal and recovery of compressed CO_2 from flue gas by a novel thermal swing chemisorption process. AIChE Journal 54, 2293–2302.

[32.] Li, J.-R., Ma, Y., McCarthy, M.C., Sculley, J., Yu, J., Jeong, H.-K., Balbuena, P.B., Zhou, H.-C., 2011. Carbon dioxide capture-related gas adsorption and separation in metal-organic frameworks. Coordination Chemistry Reviews 255, 1791–1823.

[33.] Liu, L., Deng, Q.-F., Hou, X.-X., Yuan, Z.-Y., 2012. User-friendly synthesis of nitrogen- containing polymer and microporous carbon spheres for efficient CO_2 capture. Journal of Materials Chemistry 22, 15540–15548.

[34.] Lopes, F.V.S., Grande, C.A., Rodrigues, A.E., 2012. Fast-cycling VPSA for hydrogen purification. Fuel 93, 510–523.

[35.] Martín, C.F., Plaza, M.G., Pis, J.J., Rubiera, F., Pevida, C., Centeno, T.A., 2010. On the lim- its of CO_2 capture capacity of carbons. Separation and Purification Technology 74, 225–229.

[36.] Mercel, J., Clausse, M., Meunier, F., 2006. Carbon dioxide capture by indirect thermal swing adsorption using 13X zeolite. Environmental Progress 25, 327–333. Mercel, J., Clausse, M., Meunier, F., 2008. Experimental investigation on CO_2 post-combustion capture by indirect thermal swing adsorption using 13X and 5A zeolites. Industrial and Engineering Chemistry Research 47, 209–215. Mohan, N., Kannan, G.K., Upendra, S., Subha, R., Kumar, N.S., 2009. Breakthrough of toluene vapours in granular activated carbon filled packed bed reactor. Journal of Hazardous Materials 168, 777-781

[37.] Mohanty, P., Kull, L.D., Landskron, K., 2011. Porous covalent electron-rich organoni- tridic frameworks as highly selective sorbents for methane and carbon dioxide. Nature Communications 2, 401.

[38.] P.J.M. Carrott et al. Preparation of activated carbon fibres from acrylic textile fibres Carbon (2001)

[39.] F. Stoeckli et al. Porous structure of polyarylamide based activated carbon fibres Carbon (1996)

[40.] C.W. Jones et al. Carbon molecular sieve gas separation membranes-I. Preparation and characterization based on polyimide precursors Carbon 1994.

[41.] M.C. Blanco Lopez et al. Microporous texture of activated carbon fibres prepared from Nomex aramid fibres Microporous Mesoporous Mater (2000).

[42.] M. Daley et al. Application of SO_2 onto oxidized and heat treated activated carbon fibres (ACFS) Carbon (1997)

[43.] M. Suzuki .,Activated carbon fiber: fundamentals and applications Carbon (1994)

[44.] D.D. Edie The effect of processing on the structure and properties of carbon fibres Carbon (1998)
[45.] Z. Ryu et al. Nitrogen adsorption studies of PAN-based activated carbon fibres prepared by different activation methods J Colloid Interface Sci (2000)
[46.] Z. Ryu et al. Porous structure of PAN based activated carbon fibres Carbon (1998)
[47.] T. Valdes-Solis et al. Adsorption and breakthrough performance of carbon-coated ceramic monoliths at low concentration of n-butane Chem Eng Sci (2004)
[48.] R.M. Heck et al. The application of monoliths for gas phase catalytic reactions Chem Eng J (2001)
[49.] M. Yates et al. Honeycomb monoliths of activated carbons for effluent gas purification Microporous Mesoporous Mater (2000)
[50.] D. Lozano-Castello et al. Activated carbon monoliths for methane storage: influence of binder Carbon (2002)
[51.] S. Sircar et al. Activated carbon for gas separation and storage Carbon (1996)
[52.] M.T. Kreutzer et al. Shouldn't catalysts shape up? Structured reactors in general and gas-liquid monolith reactors in particular by chemical vapor deposition and its effects on molecular sieve selectivity Catal Today (2006)
[53.] Y. Kawabuchi et al. The modification of pore size in activated carbon fibers by chemical vapor deposition and its effects on molecular seive selectivity Carbon (1998)
[54.] K.P. Gadkaree, Carbon honeycomb structures for adsorption applications Carbon (1998)
[55.] J.L. Williams, Monolithic structures, materials, properties and uses Catal Today. (2001)
[56.] D. Menard et al. Activated carbon monolith of high thermal conductivity for adsorption processes improvement part A: absorption set-up, Chem Eng Process (2005)
[57.] D. Menard et al. Development of thermally conductive packing for gas separation Carbon (2003)
[58.] T.D. Burchell et al. Passive CO2 removal using a carbon fiber Energy Consers Manage (1996)
[59.] T.D. Burchell et al. A novel carbon fibre based material and separation technology Energy Convers Manage (1997)
[60.] K.O. Kwak et al. Optimization of culture conditions for CO2 fixation by a chemoautotrophic microorganism, strain YN-1 using factorial design J Biochem Eng (2006)
[61.] K.L. Kadam Environmental implications of power generation via coal- microalgae cofiring Energy (2002)
[62.] K. Maeda et al. CO2 fixation from the flue gas on coal-fired thermal power plant by microalgae Energy Convers Manage (1995)
[63.] J.R. Benemann Utilization of carbon dioxide from fossil fuel-burning power plants with biological system Energy Convers Manage (1993)
[64.] P.H.M. Feron et al. Membrane technology in carbon dioxide removal Energy Convers Manage (1992)
[65.] E. Favre, Carbon dioxide recovery from post-combustion processes: can gas permeation membranes compete with absorption? J Memb Sci (2007)
[66.] L. Zhao et al. A parametric study of CO2/N2 gas separation membrane processes for post-combustion capture J Memb Sci (2008)
[67.] P.H.M. Feron et al. CO2 separation with polyolefin membrane contactors and dedicated absorption liquids: performances and prospects Separ Purif Tech (2002)
[68.] D. de Montigny et al. Using polypropylene and polytetrafluoroethylene membranes in a membrane contactor for CO2 absorption J Memb Sci (2006)
[69.] Corti et al. Carbon dioxide removal in power generation using membrane technology Energy (2004)
[70.] K. Li et al. Use of permeation and absorption methods for CO, removal in hollow fiber membrane modules Separ Purif Tech (1998)
[71.] R. Bounaceur et al. Membrane processes for post-combustion carbon dioxide capture: a parametric study Energy (2006)
[72.] R. Thiruvenkatachari, S. Shi Su, A.Hui and Xin Xiang Yu. "Post combustion CO2 capture by carbon fibre monolithic adsorbents." Progress in Energy and F. Khosroabadi, Aslani A., K. Bekhrad, and Z. Zolfaghari. "Analysis of Carbon Dioxide Capturing Technologies and their technology developments." Cleaner Engineering and Technology 5 (2021): 100279.
[73.] Z. Meratla Combining cryogenic flue gas emission remediation with a CO2/O2 combustion cycle Energy Convers Manage (1997)
[74.] J.T. Yeh et al. Semi-batch absorption and regeneration studies for CO2 capture by aqueous ammonia (Fuel Process Technol (2005)
[75.] S. Ma'mun et al. Selection of new absorbents for carbon dioxide capture Energy Convers Manage (2007)
[76.] D.P. Hagewiesche et al. Absorption of carbon dioxide into aqueous blends of monoethanolamine and N-methyldiethanolamine Chem Eng Sci (1995)
[77.] P.N. Dyer et al. Ion transport membrane technology for oxygen separation and syngas production Solid State Ionics (2000)
[78.] J.Y. Ren et al. Membrane-based reactive separations for power generation applications: oxygen lancing Chem Eng Sci (2003)
[79.] W. Ito et al. Oxygen separation from compressed air using a mixed conducting perovskite-type oxide membrane Solid State Ionics (2007)
[80.] S. Engels et al. Development of a zero emission coal-fired power plant by means of mixed ion conducting high temperature membranes Desalination (2006)
[81.] D.R. Vinson Air separation control technology Comput Chem Eng (2006)
[82.] A.R. Smith et al. A review of air separation technologies and their integration with energy conversion processes Fuel Process Technol (2001)
[83.] B.J.P. Buhre et al. Oxy-fuel combustion technology for coal-fired power generation (2005) Prog Energy Combust Scim (2005)

[84.] T.F. Wall ,Combustion process for carbon capture Proc Combust Inst (2007)
[85.] K. Damen et al. A comparison of electricity and hydrogen production systems with CO2 capture and storage. Part A: review and selection of promising conversion and capture technologies. Prog Energy Combust Sci (2006)
[86.] IPCC Climate change 1995: the science of climate change
[87.] IPCC Climate change 2001: the scientific basis
[88.] IPCC Climate change 2007: the physical science basis.